DYNAMIC ANALYSIS OF TYPHOON SURGES ALONG THE COASTS OF ZHEJIANG AND JIANGSU PROVINCES

CHEN CHANGSHENG (陈长胜) AND QIN ZENGHAO (秦曾灏)

(Shandong College of Oceanology, Qingdao)

ABSTRACT

Based on the numerical model shown in Ref. [1], a dynamic analysis is given for the storm surges caused by the four typhoons (i. e. typhoons Nos. 5310, 5612, 6126 and 6207) on the east coast of Zhejiang and Jiangsu Provinces, in which the contributions of various dynamic factors to local surge elevation are calculated numerically, including the Coriolis force, the atmospheric pressure force, the bottom friction, the local topography and the couple nonlinear interactions between surge current and elevation as well as between surge currents themselves. Moreover, the responses of these factors to different kinds of typhoon tracks and water depths are discussed in more detail, and the effects of grid size on the computed results demonstrated.

INTRODUCTION

In Ref. [1], much has been discussed about the nonlinear numerically computational problems of typhoon surge on the coasts of Zhejiang and Jiangsu Provinces. In order to avoid the nonlinear computational instability, a finite-difference scheme with the quadratic conservation (or the semi-momentum) was adopted. As examples, the six typhoon surges which struck the coasts of Zhejiang and Jiangsu Provinces including Shanghai have been successfully simulated. From the point of view of theoretical research, however, even with these computations, it is not sufficient to explain the main dynamic features of typhoon surge in this region. Hence, it is quite necessary to give some deeper insight into the dynamic mechanism of typhoon surge so as to derive a simpler mathematical model suitable for its prediction. According to the numerical model given in [1] (hereafter called scheme 1), a dynamic analysis is performed for the storm surges caused by the four typhoons (i. e. typhoons Nos. 5310, 5612, 6126 and 6207) on the east coasts of Zhejiang and Jiangsu Provinces. We have computed numerically the contributions of various dynamic factors in the nonlinear model to surge elevation, such as the Coriolis force, the atmospheric pressure force, the bottom friction, the local topography and couple nonlinear interactions between surge current and elevation as well as between surge currents themselves. Moreover, the responses of these factors to different kinds of typhoon tracks and water depths are discussed

Received June 10, 1984. Accepted May 23. 1985.

in more detail. In addition, the effects of grid size on the computed results are also demonstrated.

I. NUMERICAL MODEL

1. *The Finite-Difference Scheme*

The following finite-difference scheme with the quadratic conservation is employed:[1]

$$\bar{U}_t^t=-\overline{\bar{U}^x\bar{U}^x}_x-\overline{\bar{V}^y\bar{U}^y}_y+fV_{i,j}^n-g\bar{\zeta}_x^x-\frac{1}{\rho}\bar{P}_{a\,x}^x+\frac{\rho_a\nu_a^2|\,|_{i,j}^n\overline{\vec{W}W}_{x\,i,j}^n}{\rho D_{i,j}^n}-\frac{\nu_b^2|\vec{V}|_{i,j}^{n-1}U_{i,j}^{n-1}}{D_{i,j}^n},\tag{1}$$

$$\bar{V}_t^t=-\overline{\bar{U}^x\bar{V}^x}_x-\overline{\bar{V}^y\bar{V}^y}_y-fU_{i,j}^n-g\bar{\zeta}_y^y-\frac{1}{\rho}\bar{P}_{a\,y}^y+\frac{\rho_a\nu_a^2|\vec{W}|_{i,j}^nW_{y\,i,j}^n}{\rho D_{i,j}^n}-\frac{\nu_b^2|\vec{V}|_{i,j}^{n-1}V_{i,j}^{n-1}}{D_{i,j}^n},\tag{2}$$

$$\bar{\zeta}_t^t=-(\bar{D}^x\bar{U}^x)_x-(\bar{D}^y\bar{V}^y)_y.\tag{3}$$

Let α be arbitrary variable (such as U, ζ, P_a, etc) and the operators used in Eqs. (1)—(3) can be defined as:

$$\overline{\bar{U}^x\alpha_x^x}=\frac{1}{4\Delta s}[(U_{i,j+1}^n+U_{i,j}^n)(\alpha_{i,j+1}^n-\alpha_{i,j}^n)+(U_{i,j}^n+U_{i,j-1}^n)(\alpha_{i,j}^n-\alpha_{i,j-1}^n)],\tag{4}$$

$$\overline{\bar{V}^y\alpha_y^y}=\frac{1}{4\Delta s}[(V_{i+1,j}^n+V_{i,j}^n)(\alpha_{i+1,j}^n-\alpha_{i,j}^n)+(V_{i,j}^n+V_{i-1,j}^n)(\alpha_{i,j}^n-\alpha_{i-1,j}^n)],\tag{5}$$

$$(\bar{D}^x\bar{U}^x)_x=\frac{1}{4\Delta s}[(U_{i,j+1}^n+U_{i,j}^n)(D_{i,j+1}^n+D_{i,j}^n)-(U_{i,j}^n+U_{i,j-1}^n)(D_{i,j}^n+D_{i,j-1}^n)],\tag{6}$$

$$(\bar{D}^y\bar{V}^y)_y=\frac{1}{4\Delta s}[(V_{i+1,j}^n+V_{i,j}^n)(D_{i+1,j}^n+D_{i,j}^n)-(V_{i,j}^n+V_{i-1,j}^n)(D_{i,j}^n+D_{i-1,j}^n)],\tag{7}$$

$$\bar{\alpha}_x^x=\frac{1}{2\Delta s}(\alpha_{i,j+1}^n-\alpha_{i,j-1}^n),\tag{8}$$

$$\bar{\alpha}_y^y=\frac{1}{2\Delta s}(\alpha_{i+1,j}^n-\alpha_{i-1,j}^n),\tag{9}$$

$$\bar{\alpha}_t^t=\frac{1}{2\Delta t}(\alpha_{i,j}^{n+1}-\alpha_{i,j}^{n-1}),\tag{10}$$

$$D_{i,j}^n=H_{i,j}+\zeta_{i,j}^n,\tag{11}$$

$$H_{i,j}=0.25(h_{i+1,j}+h_{i-1,j}+h_{i,j-1}+h_{i,j+1}),\tag{12}$$

where $\nu^2=2.6\times10^{-3}$ and $\nu_b^2=2.0\times10^{-3}$.

2. *Computations of Atmospheric Pressure Field and Wind Field*

(1) *Distribution of atmospheric pressure*

The atmospheric pressure P_a at any grid point may be calculated by Fujita's formula as follows:

$$P_a = P_\infty - (P_\infty - P_0) \Big/ \sqrt{1+\left(\frac{r}{r_0}\right)^2}. \tag{13}$$

(2) *Distribution of wind*

Corresponding to Fujita's atmospheric pressure model, Ueno' wind field model is used for the computation of wind which may be expressed as:

$$\begin{pmatrix} W_x \\ W_y \end{pmatrix} = c_1 \begin{pmatrix} V_{x_0} \\ V_{y_0} \end{pmatrix} \exp\left(\frac{r\pi}{5\times 10^7}\right) \mp c_2 \left(\sqrt{\frac{10^3 \Delta P}{\rho_a}} \frac{1}{r_0} z^{3/2} - \frac{f}{2}\right) \left[(x_i - x_0) \begin{pmatrix} \sin 30^\circ \\ \cos 30^\circ \end{pmatrix} \right.$$
$$\left. \pm (y_i - y_0) \begin{pmatrix} \cos 30^\circ \\ \sin 30^\circ \end{pmatrix} \right], \tag{14}$$

where $z = \left[1+\left(\frac{r}{r_0}\right)^2\right]^{-\frac{1}{2}}$.

The meaning of the mathematical symbols used above is the same as those shown in Ref. [1].

II. DYNAMIC ANALYSIS

1. *Effect of the Coriolis Force*

In order to see more clearly the contributions of the Coriolis force to surge elevation under different backgrounds, the following computations are carried out:

(A) Scheme C_1 neglecting the Coriolis force throughout the whole computed region.

(B) Schemes C_2, C_3 and C_4 without the Coriolis force corresponding to the regions of depths less than (or equal to) 15, 25 and 50 m, respectively.

(1) *Effect of the Coriolis force on surge elevation*

Table 1

$f=0$ (°/ hr)

Station / Typhoon No	Haimen		Zapu		Wusong	
	$\Delta\zeta_{max}$	ΔT_{max}	$\Delta\zeta_{max}$	ΔT_{max}	$\Delta\zeta_{max}$	ΔT_{max}
5612	11	2	17.6	1	32.9	1
6207	*	*	46.8	−2	11.1	0

$\Delta\zeta_{max}$ The percentage of the absolute value of the difference between the maximum surge elevations obtained from scheme C_1 and scheme 1 respectively relative to the peak surge given by scheme 1.

ΔT_{max} The difference of time of peak surge arrival obtained by scheme C_1 relative to that given by scheme 1.

* The phase of surge elevation obtained by scheme C_1 is opposite to that given by scheme 1.

Taking the two representative typhoons (Nos. 5612 and 6207) with different kinds of tracks as examples, in Figs. 1 and 2, curves 1 and 2 illustrate the time variations of surge elevation obtained from scheme 1 and scheme C_1, respectively. Table 1 indicates the differences of maximum surge elevation and its time of occurrence obtained by C_1 relative to those given by scheme 1. The main features are as follows:

1) The surge elevations obtained from scheme C_1 deviate greatly from those from scheme 1. For all the typhoon surge processes , the maximum difference between them at each station exceeds 50 cm.

2) The differences between the maximum surge elevations as well as between their times of occurrence obtained by the above schemes, respectively, differ considerably from each other for different kinds of typhoon tracks. Except for Wusong , these differences are greater in the alongshore-travelling typhoon (No. 6207) than in the landfalling typhoons (Nos. 5310 5612 and 6126). Moreover, the former appears negative while the latter positive, that is, in the alongshore-travelling tyhoon, the peak surge and its time of occurrence given by scheme C_1 are respectively smaller and earlier than that given by scheme 1, but the opposite is true for the landfalling typhoons.

3) The trends of variation of surge elevations obtained by the above two schemes are analogous to each other except at Haimen during the passage of typhoon No. 6207.

It should be pointed out that during the period of typhoon No. 6207, the opposite phases appear in surge elevation obtained from either scheme C_1 or scheme 1 at Haimen. This means that the Coriolis force has a greater effect not only on the enhancement of typhoon surge, but also on its variation trend.

(2) *Variation of the Coriolis effect with depth*

Table 2

$h \leqslant 15$m, 25m, 50m, $f = 0$ (% hr)

Typhoon No.	5612						6207					
Station	≤15m		≤25m		≤50m		≤15m		≤25m		≤50m	
	$\Delta\zeta_{max}$	ΔT_{max}	$\Delta\zeta_{max}$	ΔT_{max}	$\Delta\zeta_{max}$	ΔT_{max}	$\Delta\zeta_{max}$	ΔT_{max}	$\Delta\zeta_{max}$	ΔT_{max}	$\Delta\zeta_{max}$	ΔT_{max}
Haimen	0.6	0	3.1	0	13.5	0	6.3	0	22.8	0	69.6	0
Zapu	0.8	0	3.3	0	5.3	1	0.7	0	28.1	−2	33.8	−2
Wusong	0.9	0	8.2	0	16.4	1	2.1	0	11.7	−1	12.2	−1

$\Delta\zeta_{max}$ The percentage of the absolute value of difference between the maximum surge elevation obtained from schemes C_2, C_3 and C_4 respectively and that given by scheme 1 relative to the peak surge given by scheme 1.

ΔT_{max} The time difference of the maximum surge elevation obtained by schemes C_2, C_3, and C_4 respectively, relative to that given by scheme 1.

Table 2 indicates the differences of the maximum surge elevation obtained from schemes C_2, C_3 and C_4, respectively, and their times of occurrence relative to those given by scheme 1. The following conclusions may be drawn from the computations:

1) The variation of the Coriolis effect on surge elevation with depth is greater in the alongshore typhoon process than in the landfalling typhoon processes, as mentioned above.

2) The Coriolis effect becomes stronger as the water depth is increasing. In the shallow-water region whose depth is less than 15 m, the Coriolis force gives little contribution to the maximum surge elevation at any station and may therefore be omitted. This result agrees fairly well with the conclusion given by the scale analysis in [2] an [3]. When the depth increases to 25 m, i.e. in the sea region of depth less than (or equal to) 25 m, it must be careful to treat the Coriolis force. Its contribution to the maximum surge elevation generated by the alongshore-travelling typhoon could no longer be negligible, though small in the landfalling typhoons. Undoubtedly, in the sea region with a depth greater than 25 m, the Coriolis effect must be retained.

(3) *The f-plane and the β-plane approximations*

Table 3

f and β Effects (cm %)

Station / Typhoon No.	Haimen				Zapu				Wusong			
	F_1	F_2	G_1	G_2	F_1	F_2	G_1	G_2	F_1	F_2	G_1	G_2
5612	5	3.1	1	0.6	4	1	1	0.3	5	2.3	1	0.5
6207	10	12.7	1	1.3	10	7.2	2	1.4	15	18	3	3.8

F_1 The absolute value of the maximum difference between the surge elevations obtained from the scheme with f-plane approximation and scheme 1 respectively.

G_1 The absolute value of the maximum difference between the surge elevations obtained from the scheme with β-plane approximation and scheme 1 respectively.

F_2 The percentage of F_1 relative to the peak surge given by scheme 1.

G_2 The percentage of G_1 relative to the peak surge given by scheme 1.

In this paper, on the f-plane, the Coriolis term f is given by $f=2\ \omega\ \sin 30°$ while on the β-plane, $f=2\omega\sin 26°+y\left.\frac{\partial f}{\partial y}\right|_{\theta=26}$. For example, Table 3 shows the effects of the f-plane and β-plane approximations on the surge elevation, respectively. It is evident that the difference in surge elevation caused by the f-plane approximation is greater in the alongshore-travelling typhoon process than in the landfalling typhoon process, the maximum value of which is 15 cm (at Wusong during the peroid of typhoon No. 6207). The maximum difference caused by β-effect is 3 cm. This implies that the maximum correction of β-effect to the f-plane approximation in this region is only about 10 cm. In general, for the

computational region we chose, the effect of the variation of the Coriolis parameter with latitude on maximum surge elevation is small and may therefore be neglected. The *f*-plane approximation is sufficient enough to ensure the accuracy of numerical computation.

2. *Couple Nonlinear Interaction Between Surge Currents Themselves*

Table 4

$\vec{V}\cdot\nabla\vec{V}=0$ (cm %)

Station / Typhoon No.	Haimen		Zapu		Wusong	
	$\Delta\zeta_{max}$	*PR*	$\Delta\zeta_{max}$	*PR*	$\Delta\zeta_{max}$	*PR*
5612	2	1.2	1	0.3	3	1.4
6207	5	6.3	1	0.7	1	1.2

$\Delta\zeta_{max}$ The absolute value of the maximum difference between surge elevation obtained from either the scheme without the nonlinear advective term or scheme 1.

PR The percentage of $\Delta\zeta_{max}$ relative to the peak surge given by scheme 1.

Table 4 indicates the contribution of the nonlinear advective term in the numerical model to the maximum surge elevation. It is obvious that the effect of the couple nonlinear interaction between surge currents themselves is so small that it can be safely disregarded, no matter what kind of track the typhoon takes. Ignoring the nonlinear advective term, we can not only avoid taking the nonlinear computational instability into account, but also provide conveniently a simple linear model to predict the typhoon surge on the coasts of Zhejiang and Jiangsu Provinces.

3. *Couple Nonlinear Interaction Between Surge Current and Elevation*

Table 5

$\vec{V}\cdot\nabla\zeta=0$ (cm %)

Station / Typhoon No.	Haimen				Zapu				Wusong			
	ΔI	*I*	ΔJ	*J*	ΔI	*I*	ΔJ	*J*	ΔI	*I*	ΔJ	*J*
5612	3	1.8	2	1.2	17	4.3	3	0.8	2	0.9	1	0.5
6207	4	5.1	3	3.8	17	12.2	2	1.4	7	3.7	2	1.1

ΔI The absolute value of the maximum difference of the surge elevation obtained by the scheme without the nonlinear term comprising surge current and elevation relative to that given by scheme 1.

ΔJ The absolute value of the maximum difference of the surge elevation obtained by the scheme without the nonlinear interaction term comprising surge current and elevation corresponding to the region with a depth greater than 15 m relative to that given by scheme 1.

I The percentage of ΔI relative to the peak surge given by scheme 1.
J The percentage of ΔJ relative to the peak surge given by scheme 1.

In Fig. 1, curve 3 illustrate the variation of surge elevation with time obtained from the scheme ignoring the couple nonlinear interaction between surge current and elevation. Table 5 indicates the contributions of this nonlinear interaction under different backgrounds to surge elevation. Computations show that the couple nonlinear interaction between surge current and elevation has less influence on the trend of variation of surge elevation, its magnitude being closely related to the water depth and surge elevation (the conclusion is similar to that in [2]). As a result, its effect is more remarkable near the peak surge and is thus greater at stations located inside the Hangzhou Bay than that outside the Bay. In the sea region with a depth greater than 15 m, the contribution of this nonlinear interaction to the maximum surge elevation is nearly 1/100, and can therefore be neglected. In addition, this nonlinear effect is much weaker in the landfalling typhoon process than in the alongshore travelling typhoon process.

4. *Effect of the Atmospheric Pressure Force*

In order to analyse the contribution of the atmospheric pressure force to the surge elevation under different backgrounds more clearly, the following computations are made:

(A) Scheme P_1 neglecting the atmospheric pressure force throughout the whole computational region.

(B) Scheme P_2 without taking account of the atmospheric pressure force corresponding to the sea region with a depth less than 50 m.

Table 6

Effect of Atmospheric Pressure Force (cm %)

Station / Typhoon No.	Haimen				Zapu				Wusong			
	$\nabla P_a=0$	$\zeta=\frac{P_a}{\rho g}$	$h<50$m, $\Delta P_a=0$		$\nabla P_a=0$	$\zeta=\frac{P_a}{\rho g}$	$h<50$m, $\nabla P_a=0$		$\nabla P_a=0$	$\zeta=\frac{P_a}{\rho g}$	$h<15$m, $\nabla P_a=0$	
	$\Delta\zeta_p$	$\Delta\zeta_{sp}$	$\Delta\zeta_p$	N_p	$\Delta\zeta_p$	$\Delta\zeta_{sp}$	$\Delta\zeta_p$	N_p	$\Delta\zeta_p$	$\Delta\zeta_{sp}$	$\Delta\zeta_p$	N_p
5612	87	63	9	5.5	52	40	25	6.3	36	28	13	5.9
6207	7	6	1	1.3	4	9	5	6.3	8	12	6	7.6

$\Delta\zeta_p$ The absolute value of the maximum difference of surge elevation obtained by either scheme P_1 or scheme P_2 relative to that given by scheme 1.
N_p The percentage of $\Delta\zeta_p$ relative to the peak surge given by scheme 1.
$\Delta\zeta_{sp}$ The maximum surge height caused by process pressure drop through "inverted barometric effect".

In Fig. 1, curve 4 illustrates the variation of surge elevation with time obtained from scheme P_1. Table 6 indicates the difference between surge elevations obtained from eigher scheme P_1 or scheme 1 as well as the maximum surge height caused by process pressure drop

through "inverted barometric effect". We can see from these figures and the table that it has less influence on the trend of variation of surge elevation whether the atmospheric pressure force exists or not. The maximum difference of surge elevation at stations caused by the scheme P_1 is directly proportional to the process pressure drop and often occures near the peak surge, i. e. during all the typhoon's passages, the greater the atmospheric pressure at certain station falls, the more remarkable the difference appears. We can easily find that both $\Delta\zeta_p$ and $\Lambda\zeta_{sp}$ are comparable in the order of magnitude, but unequal. In a very extreme case, the former is twofolds as much as the latter (at Haimen during the period of typhoon No. 5310). Hence, the atmospheric pressure 's effect can not be simple relaced by the hydrostatic pressure's effect in the problem of typhoon surge. On the other hand, the effect of atmospheric pressure force on surge height would become more intensive with an increasing depth. Its ratio of increase is inversely proportional to the process pressure drop. In the computed sea region with a depth less than 50 m, when the process pressure drop is smaller, the contribution of atmospheric pressure force to the maximum surge height is about 1/100 and may thus be negligible; when it becomes larger, its contribution is important to the first approximation.

5. *Effect of the Bottom Topography*

As mentioned in [1], the configuration of the whole computed region is rather complicated. Roughly speaking, the sea bottom topography rises northwestward continuously with a larger slope in the direction normal to the coast than that parallel to the coast. For the sake of comparison with the storm surge on the continental shelf with the slope normal to the coast alone, the effect of the bottom topographic slope parallel to the coast on typhoon surge is here discussed in more detail.

Table 7

Effect of the Sea Bottom Topography (cm %)

Station / Typhoon No.	Haimen		Zapu		Wusong	
	$\Delta\zeta_b$	N_b	$\Delta\zeta_b$	N_b	$\Delta\zeta_b$	N_b
5612	40	24.5	213	54.2	132	60.3
6207	90	113.9	106	76.3	88	46.8

$\Delta\zeta_b$ The absolute value of the maximum difference between surge elevation obtained from either scheme B or scheme 1.

N_b The percentage of $\Delta\zeta_b$ relative to the peak surge given by scheme 1.

In Fig. 1, curve 5 illustrates the time history of the surge elevation obtained from the scheme without the bottom topographic slope parallel to the coast (scheme B). Table 7

indicates the difference of the surge elevation obtained by scheme B relative to that obtained by scheme 1. Computations show that the effect of the sea bottom topography on typhoon surge is rather remarkable. The surge elevation obtained by scheme B deviates greatly from that given by scheme 1. For example, during the period of strong typhoon No. 5612, the maximum difference between them at Ganpu reaches 234 cm. Although the maximum difference at Haimen during the typhoon No. 6207 is only 90 cm, it exceeds 13.9 percent of the maximum surge elevation given by scheme 1. It follows that the slope of the bottom topography parallel to the coast plays a very important role in the typhoon surges on the east coasts of Zhejiang and Jiangsu Provinces apart from the one normal to the coast. This is one of main distinctions between the typhoon surge in this region and the storm surge on the continental shelf with a slope normal to the coast alone.

6. *Effect of Bottom Friction*

(1) *The quadratic law of bottom friction*

In Fig. 1, curve 6 illustrates the time history of surge elevation without the bottom friction. Comparing it with curve 1, we can see that the coastal surge generated by a landfalling typhoon is insensitive to the bottom friction. The opposite is true for the coastal surge generated by an alongshore-travelling typhoon, where the computations without bottom friction lead to the surge distortion and the numerical instability. Therefore, as far as the storm surge generated by an alongshore-travelling typhoon is concerned, the bottom friction must be retained.

(2) *Linear bottom friction*

The choice of bottom friction formulation is essential for the shallow water dynamics. In general, bottom stress can be evaluated from the depth-mean current using either a linear or nonlinear formula of bottom friction. The possibility of quadratic frictional law for typhoon surges on the Zhejiang and Jiangsu Provinces has been confirmed in [1] by means of numerical computation. Can a linear formula of bottom friction be used to simulate a typhoon surge in this region? It is the intention of the present paper to answer the question by numerical tests ot a certain extent.

The following linear bottom frictional formula is adopted:

$$\tilde{\tau}_b = \nu \vec{V}, \tag{15}$$

where the coefficient ν equals 5.0×10^{-2} cm^2/sec.

As an example, the numerical scheme with the linear bottom frictional formula given by Eq. (15) is tested for the storm surge generated by the alongshore typhoon No. 6207 (see curve 7 in Fig. 1b). As a result, the computed surge at Wusong undergoes serious distortion, so that the whole computation at this station ends with failure. It is noteworthy that in this computation the value of ν ($\sim 10^{-2}$ cm^2/sec) has been exaggerated. It follows that at least the linear bottom frictional formula is not adaptable to some stations where the nonlinear

interaction between the currents themselves is very important in its effect of bottom friction on surge elevation.

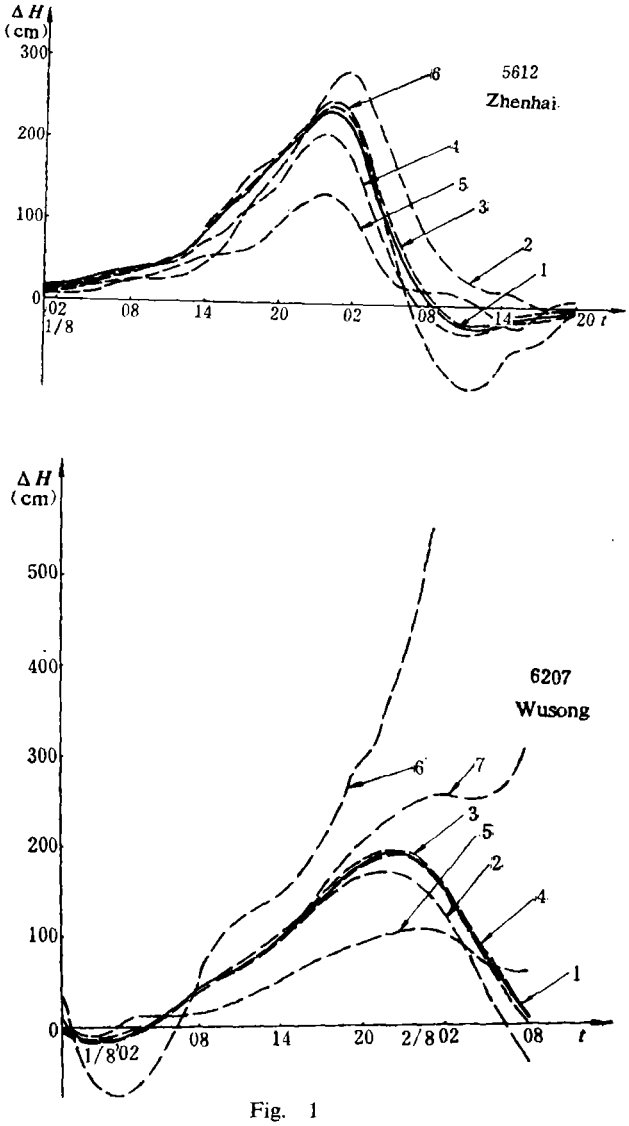

Fig. 1

1 — The time variation of surge elevation given by scheme 1;
2 — The time variation of surge elevation given by scheme C_1;
3 — The time variation of surge elevation given by the scheme ignoring coupie nonlinear interactino between surge current and elevation;
4 — The time variation of surge elevation given by scheme P_1;
5 — The time variation of surge elevation given by scheme B;
6 — The time variation of surge elevation without the bottom friction;
7 — The time variation of surge elevation with the linear bottom friction.

III. NESTED-GRID MODEL

In order to give some further insight into the effect of the choice of grids on the computed results, the nested-grids shown in Fig. 2 are employed, in which the coarse and fine grid

sizes are taken to be 30 km and 15 km respectively. According to the numerical model given in [1], for example, the storm surge generated by the strong typhoon No. 5612 is computed numerically by using the above nested-grid model.

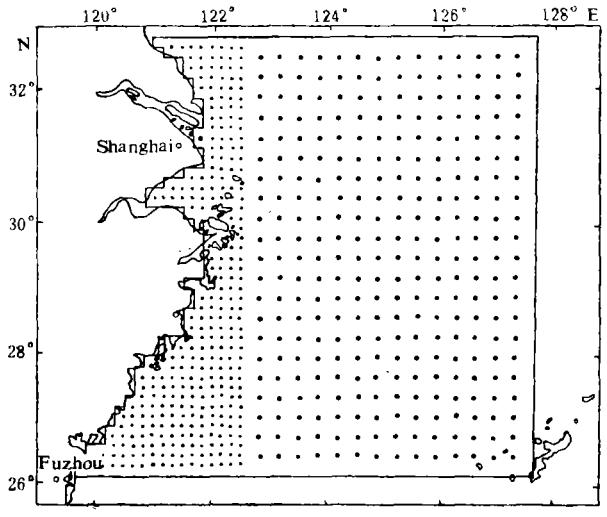

Fig. 2. Nested-grids.

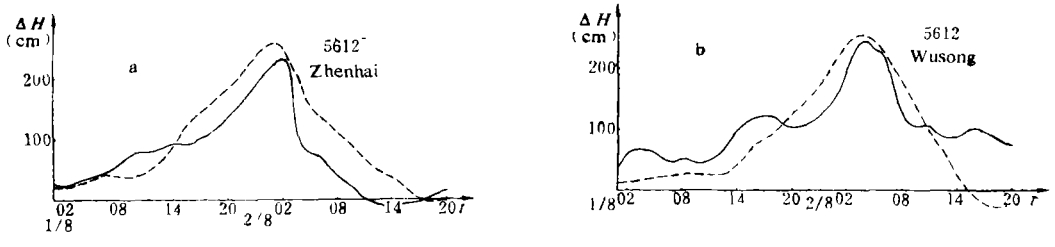

Fig. 3. Comparison between the computed and observed surge.
---- computed; —— observed.

Fig. 3 illustrates the comparisons between the observed and computed surges at two selected stations. As we can see, the computed surges are in good agreement with observations. In comparison with the computed surge obtained by scheme 1 (i. e. the coarse-grid model), the phase difference of the computed peak surge relative to observed one is smaller in the nested-grid model than in scheme 1. At Wusong, the time of occurrence of the computed peak surge is in accordance with the observations. Hence the nested-grid model is more effective than the coarse-grid one in consideration of the simulations of the peak surge and its time of arrival. This implies that one of the errors caused by numerical computation might come from the choice of grids.

IV. CONCLUSIONS

From the foregoing analyses, we might conclude as follows:

(1) The Coriolis effect on typhoon surge is more important in the alongshore-travelling typhoon than in the landfalling typhoon. In the shallow water region of depth less than 15 m, this effect is negligibly small.

(2) The couple nonlinear interaction between the surge currents themselves is so small that it can be omitted.

(3) The contribution of the couple interaction between surge current and elevation to the maximum surge elevation is related to the tracks of typhoon. This effect is of minor importance and be safely omitted for the zeroth-order approximation.

(4) The effect of the atmospheric pressure force on typhoon surge is important when the process pressure drop is comparatively large, otherwise it may be neglected.

(5) The slope of bottom topography parallel to the coast plays a very important role in the development of typhoon surges on the east coasts of Zhejiang and Jiangsu Provinces.

(6) The bottom frictional effect on typhoon surges is highly important for the alongshore-travelling typhoon and the opposite holds true for the landfalling typhoon.

(7) The quadratic law of bottom friction fits in general better than the linear one which can not be used to calculate typhoon surge for some ports under the actual conditions.

(8) It is helpful to reduce the errors between the computed time of peak surge arrival and the observation by introducing the nested-grid model.

REFERENCES

[1] Chen Changsheng & Qin Zenghao, *Advances in Atmospheric Science*, **2**(1985), 1: 8—19.
[2] Chin Tsenghao (Qin zenghao) and Feng Shihzao (Feng Shizuo), *Scientia Sinica*, **18**(1975), 2: 241—261.
[3] 冯士筰, 风暴潮导论, 科学出版社, 1982, 241.
[4] Kielman, J. and Z. Kowalik, *Oceanologica Acta*, **3**(1980), 2: 51—58.